

Sub-Sub- T_g Enthalpy Relaxation in a B_2O_3 Glass

H. S. CHEN and C. R. KURKJIAN*

Bell Laboratories, Murray Hill, New Jersey 07974

Enthalpy relaxation processes in a B_2O_3 glass were investigated calorimetrically in the temperature region from well below to near the glass-transition temperature T_g . The low-temperature ($T_a < T_g - 100$ K) or sub-sub- T_g anneals stabilize the glass structure. On heating, the annealed sample shows an excess endothermic peak above the annealing temperature T_a , and gradually recovers the original enthalpy without heating through T_g . The enthalpy relaxation evolves in a continuous manner with annealing time as seen in the recovery process. As T_a approaches T_g , a gradual transformation of the sub-sub- T_g behavior to that characteristic of the sub- T_g anneal occurs. The relaxation spectrum exhibits a broad distribution of relaxation times with activation energies of $\sim 10^5$ J/mol. The so-called β distribution commonly used in the analysis of the sub- T_g relaxation processes is seen to be too narrow to describe the sub-sub- T_g behavior. Possible mechanisms for the sub-sub- T_g relaxation phenomena are proposed.

I. Introduction

IN PREVIOUS papers,¹⁻⁴ structural relaxations at temperatures well below the glass-transition T_g (sub-sub- T_g) were studied calorimetrically and dilatometrically. These relaxations are characterized by complete recovery of the enthalpy and volume of the annealed sample without reheating through T_g and continuous development of recovery spectra with annealing time and temperature. In these earlier works both metallic and polymeric glasses were studied and, despite extreme chemical, physical, and structural differences, remarkable similarities were found in their low-temperature relaxation behavior. To date, however, no work on these so-called sub-sub- T_g relaxations has been reported in inorganic oxide glasses.

In this paper we report calorimetric data for glassy B_2O_3 . This material is particularly attractive because it is quite different from the polymeric and metallic glasses studied earlier in that it is a covalent, single-oxide, network glass with T_g in a range accessible to commercial scanning calorimeters. Although it is sensitive to reaction with water, reasonable experimental precautions can overcome this problem. In addition to its low-temperature character, B_2O_3 is of interest from the point of view of its specific heat and relaxational behavior. Although few specific heat data are generally available for oxide glasses, boron oxide has been rather carefully studied from the first work of Thomas and Parks in 1931⁵ to several very recent works.^{6,7} In addition, as pointed out by Moynihan,⁸ B_2O_3 is the only oxide glass-former for which pressure-volume, temperature-volume, and temperature-enthalpy relaxations have been studied. Also, viscous flow⁹ and internal friction^{10,11} have been studied by many investigators, and thus a substantial amount of background information is available on this material.

II. Experimental Procedure

(1) Sample Preparation

The glass was prepared by melting reagent-grade boric acid in a platinum crucible at 1300°C while bubbling N_2 through the melt. The water content was estimated by ir absorption¹² to be ≈ 0.05 mol%. The melt was cast into sheets ≈ 1 mm thick. The

glassy samples were then stored in a dry-box. For calorimetric measurements, B_2O_3 glassy samples ≈ 2.5 mm square by 1 mm thick were sealed with Al sample container and placed in a borosilicate glass* tube. The encapsulated samples were then evacuated for 1 h and refilled with dry nitrogen.

(2) Calorimetric Measurements

The apparent specific heat, C_p , was measured with a differential scanning calorimeter.[†] Care was taken to reduce the thermal drift by prewarming the instrument for at least 5 h in the temperature range of interest. The samples weighed ≈ 15 mg. The accuracy of the data was ≈ 0.04 J/g·K for the absolute values, but was > 0.02 J/g·K for the relative C_p , or ΔC_p measurements. Prior to each measurement, the samples were thermally conditioned in the calorimeter at 620 K (≈ 40 K above the glass transition T_g) for 2 min and cooled to 320 K at predetermined rates ranging from 0.31 to 160 K/min. The thermally conditioned samples were then annealed in situ at various temperatures for up to 30 h. In a few cases, longer anneals, up to 400 h, were performed in a well-controlled furnace after placing the encapsulated sample inside a vacuum-sealed borosilicate glass* tube.

Following the annealing treatment, the sample was thermally scanned at a certain rate (depending on the purpose of the measurement) from 320 to 620 K to obtain the C_p data of the annealed sample. It was then cooled to 320 K and reheated immediately to obtain the C_p data of the "reference" sample ($C_{p,r}$). The cooling and heating rates were now fixed at 20 K/min. The difference in $C_p(T)$ and $C_{p,r}(T)$ was used to monitor the structural-relaxation process. This test procedure is essential to eliminate any possible scatter that might result from drift in the calorimeter due to the prolonged annealing, and to enable small differences in C_p to be measured.

III. Results

(1) Effects of Cooling Rate

A typical set of C_p data is shown in Fig. 1. The data were taken at a heating rate $\alpha_h (=dT/dt)$ of 20 K/min on a sample cooled from 620 K at the rates (α_c) indicated in the figure. The sample with faster cooling than heating rate ($\alpha_c = 80$, $\alpha_h = 20$) shows C_p values lower than the reference values, $C_{p,r}(T)$, for $T \geq 480$ K. The negative values of $\Delta C_p (=C_p - C_{p,r})$ can be understood as a result of structural stabilization of the faster-cooled sample, which has a higher fictive temperature T_f . The sample with slower-cooling rate α_c of 5 K/min shows a C_p behavior which closely follows the $C_{p,r}$ curve up to ≈ 480 K, then exhibits an excess endothermic specific heat, i.e. positive ΔC_p , at higher temperature. The temperature $T^* = 480$ K, at which C_p departs from $C_{p,r}$, is well below the glass-transition temperature $T_g = 583$ K (at $\alpha_h = 20$ K/min) where T_g is defined as the point of inflection in the C_p vs T curve. If the cooling rate is slow enough, as for example in the sample with the slowest cooling rate of $\alpha_c = 0.31$ K/min, a pronounced C_p peak is shown only in the glass-transition region. This behavior has been commonly observed for sub- T_g annealed glassy samples and is interpreted as a result of retarded atomic mobility.

In all cases above T_g ($T \geq 610$ K), C_p values fall on the equilibrium liquid value

$$C_{p,e} = 1.88 \text{ J/g}\cdot\text{K} \quad (1)$$

which is seen to be temperature-independent. The glass specific

Presented at the Glass Division Fall Meeting, Bedford, Pennsylvania, October 14, 1981 (Paper No. 7-G-81F). Received September 13, 1982; revised copy received March 4, 1983; approved May 5, 1983.

*Member, the American Ceramic Society.

*Pyrex, Corning Glass Works, Corning, NY.

†DSC-2, Perkin-Elmer Corp., Norwalk, CT.

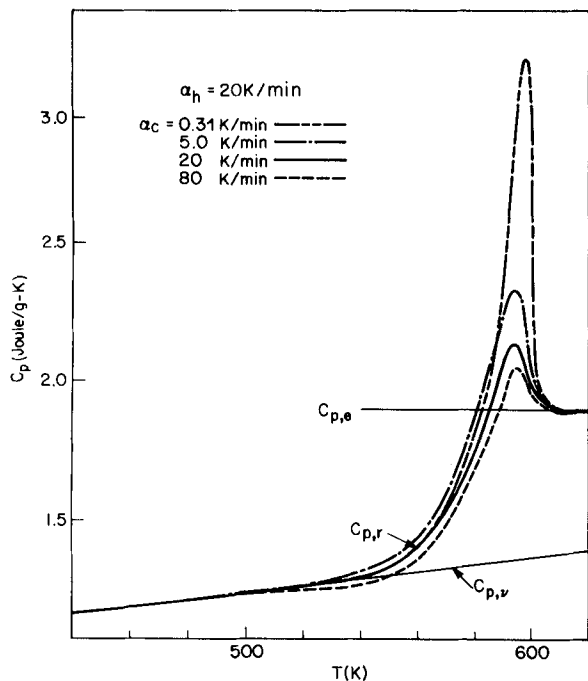


Fig. 1. Specific heats of B_2O_3 glass sample cooled from 620 K through T_g to room temperature at rates (α_c) indicated; rate of measurement (α_h) = 20 K/min.

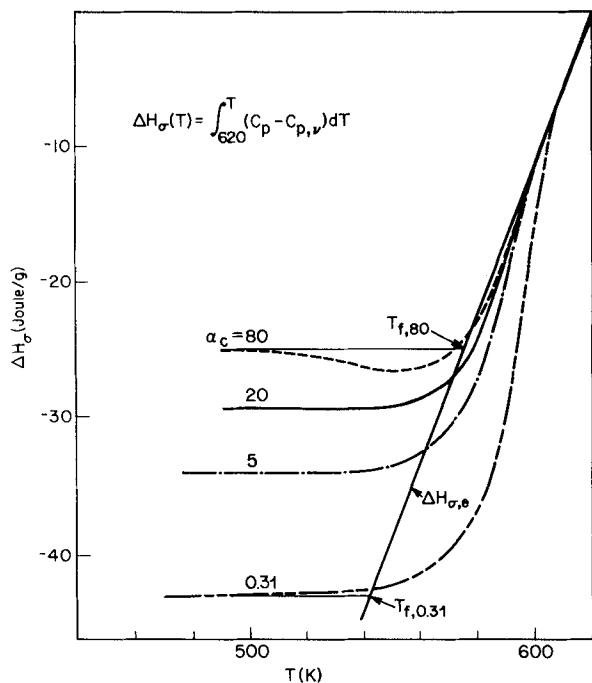


Fig. 2. Configurational enthalpy, $\Delta H_\sigma(T)$, of samples corresponding to Fig. 1. Fictive temperature, T_{f,α_c} , is determined as shown in figure.

heat, or the vibrational specific heat which was extrapolated from C_p values in the low-temperature region $T \leq 420$ K, is a linear function of temperature such that

$$C_{p,v} = 1.13 + 1.25 \times 10^{-3}(T - 420) \text{ J/g}\cdot\text{K} \quad (2)$$

These values are similar to those found by DeBolt *et al.*⁷ Figure 2 shows the configurational enthalpy $\Delta H_\sigma(T)$ of the samples corresponding to Fig. 1. Here $\Delta H_\sigma(620 \text{ K}) = 0$ is taken as a reference, and the configurational enthalpy is expressed by:

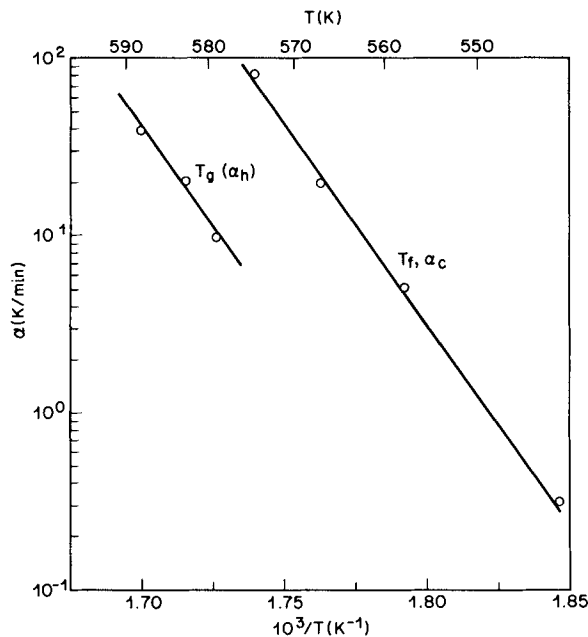


Fig. 3. Fictive temperatures obtained in Fig. 2 and measured glass transition temperature, $T_g(\alpha_h)$.

$$\Delta H_\sigma(T) = \int_{620}^T (C_p - C_{p,v}) dT' \quad (3)$$

and, accordingly, $(\Delta H_\sigma - \Delta H_{\sigma,e})$ represents the unrelaxed configurational enthalpy of the glassy samples, where $\Delta H_{\sigma,e}$ is the ΔH_σ of the equilibrium liquid. On cooling through the transition region, the glass eventually attains, at $T \leq 480$ K, a constant limiting $\Delta H_{\sigma,g}(\alpha_c) = \Delta H_{\sigma,e}(T_{f,\alpha_c})$ shown in Fig. 2. Here T_{f,α_c} are fictive temperatures of the glass samples. Figure 3 plots the evaluated T_{f,α_c} as a function of the logarithm of the prior cooling rate, α_c , of the sample. For comparison, the change in the measured glass-transition temperature $T_g(\alpha_h)$ with rate of heating is also shown in Fig. 3. The detailed measurement of $T_g(\alpha_h)$ will be elaborated in Section III(3). Both the $T_f(\alpha_c)$ and $T_g(\alpha_h)$ measurements yield an apparent activation energy $Q_a \approx 4.5 \times 10^5$ J/mol.

Figures 1 and 2 reveal two significant features; first, $\Delta H_\sigma(T)$ remains at a constant value up to 420 K and then, depending on prior cooling rate, decreases (for $\alpha_c = 80$ K/min) or increases (for $\alpha_c = 20, 5$, and 0.31 K/min) above 480 K, which is well below T_g . Thus B_2O_3 glass exhibits a very fast, probably localized relaxation process (see Section III(4)) as compared with the cooperative relaxation responsible for the glass transition, and the stabilization of the glass near the transition does not appear to eliminate the very short-time relaxation processes. Second, in all cases the $\Delta H_\sigma(T)$ curves cross the equilibrium $\Delta H_{\sigma,e}(T_f = T)$ with positive slope, and eventually approach equilibrium at high temperature from below the equilibrium curve. The relaxation behavior, moving away from equilibrium with increasing time in the region below T_f , is a manifestation of the memory effect and clearly confirms the necessity of a distribution of relaxation times to describe the structural state of a glass.^{6,7}

(2) Annealing Behavior

To further explore the kinetics of these relaxation processes, the samples were systematically subjected to annealing in two temperature regions: a sub-sub- T_g region, e.g. $T_a < T_g - 100$ K, and a sub- T_g region.

(A) *Sub-Sub- T_g Anneals*: Typical thermograms of fast-cooled ($\alpha_c = 80$ K/min) B_2O_3 are shown in Fig. 4(A). After annealing at 420 K for 30 h (curve 2), the sample exhibits an excess endothermic reaction ($\Delta C_p = C_p - C_{p,r} > 0$) above $T_a = 420$ K and peaking at T_m (≈ 525 K). ΔC_p then decreases and is followed by a broad exothermic peak ($\Delta C_p < 0$) which merges at $T \approx 575$ K with the thermogram (curve 1) of the as-cooled sample, which has had no

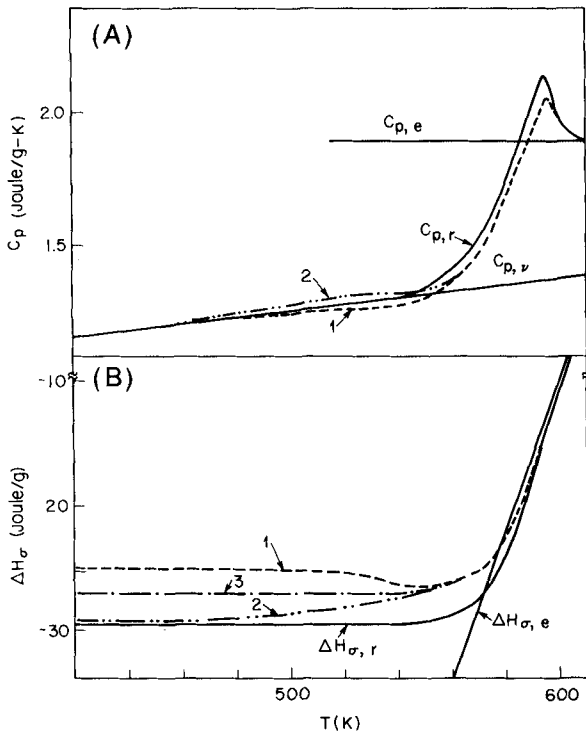


Fig. 4. Thermograms of fast-cooled ($\alpha_c=80$ K/min) B_2O_3 glass subjected to further annealing at 420 K for 30 h. (A) Apparent specific heats, C_p , and (B) configurational enthalpy, ΔH_σ . All designations are the same as in Figs. 1 and 2; $\alpha_h=20$ K/min.

further anneal. If the annealed sample is scanned to T_m' , then cooled to 320 K, on reheating the endothermic peak diminishes and C_p falls on $C_{p,r}$ for $T \leq T_m'$ and then at higher temperatures follows the same exothermic reaction (curve 3, not shown in Fig. 4(A)). Corresponding $\Delta H_\sigma(T)$ curves are shown in Fig. 4(B). Clearly the endothermic reaction ($\Delta H_{\sigma,3} - \Delta H_{\sigma,2}$) is recoverable, whereas the stabilization leading to the exothermic reaction ($\Delta H_{\sigma,1} - \Delta H_{\sigma,3}$) is irrecoverable.

Figure 5 shows the thermograms and $\Delta H_\sigma(T)$ of samples annealed at 420 K for 30 h after prior cooling through T_g at $\alpha_c=20$ K/min. In Fig. 5(A) the heating curve shows a C_p behavior which follows closely the data of the reference sample $C_{p,r}$ up to $T_a=420$ K, then exhibits an endotherm relative to the reference sample before merging again below T_g . Consequently, $-\Delta H_\sigma$ of the annealed sample (Fig. 5(B)) increases toward that of the unannealed sample and merges with it before T_g . This implies that, as a result of structural relaxation which occurred during the low-temperature anneal, it is possible to recover the initial structure of glass without reheating it through the glass transition. The $-\Delta H_\sigma(T)$ curves thus tend to stay to the left of the equilibrium line with increasing time. These features differ from the phenomena commonly observed in the usual sub- T_g anneal for glassy materials.

To illustrate more clearly the evolution of enthalpy relaxation, the difference between C_p and $C_{p,r}$ (ΔC_p) is shown in Fig. 6. It was earlier noted that the endothermic C_p peak always begins to rise at $T_a=420$ K, regardless of the duration of the annealing, and that it evolves in a continuous manner indicative of a continuous relaxation spectrum. It is seen in Fig. 6 that the magnitude of the endothermic peak is greater for the sample with faster prior cooling. This suggests that the more disordered the state the more intense is the short-time relaxation. This is in harmony with the diminishing ΔC_p (for $T < T_g$) of the slowly cooled ($\alpha_c=0.31$ K/min) sample mentioned previously (Fig. 1). Both peak temperatures T_m' and T_m increase approximately as the logarithm of annealing time t_a (Fig. 7). Although the slope has units of activation energy, it has no physical meaning because of a broad distribution in activation energy, as will be shown later.

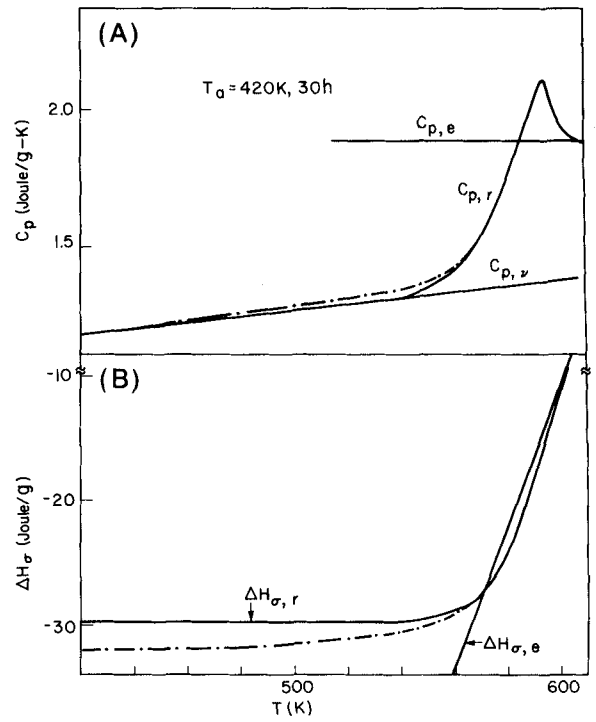


Fig. 5. As in Fig. 4, except that prior cooling rate, α_c , was 20 K/min.

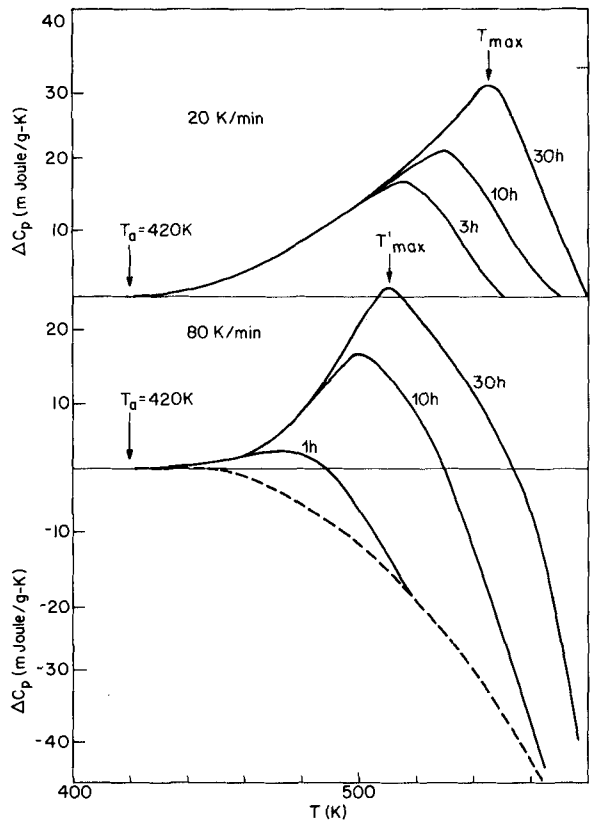


Fig. 6. Difference in specific heat, ΔC_p ($\equiv C_p - C_{p,r}$) of B_2O_3 samples as a function of annealing time, t_a .

The same calorimetric behavior found for the sample annealed at 420 K is seen for samples annealed at higher temperatures. The endothermic reaction, however, sets in at $T=T_a$. This phenomenon becomes less pronounced as T_a is increased to near T_g and, depending on the length of annealing time, a second C_p peak appears

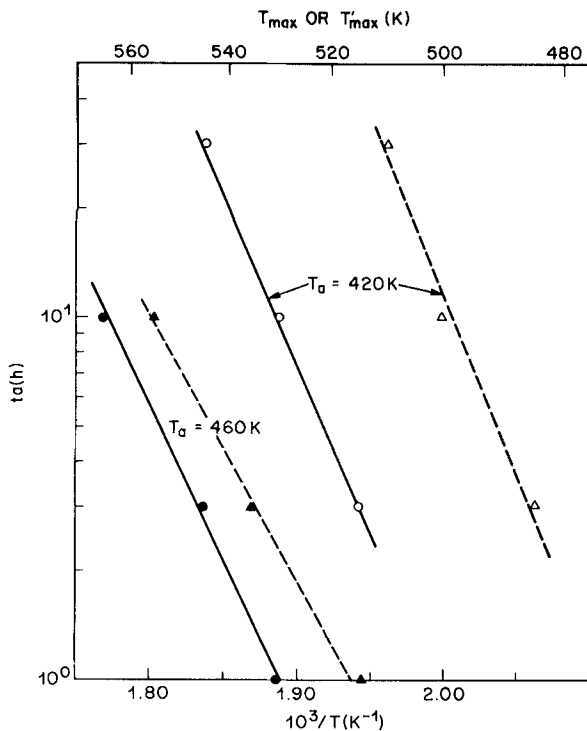


Fig. 7. Development of specific heat peak temperatures (O) T_m and (Δ) T_m' with t_a , at $T_a=420$ and 460 K.

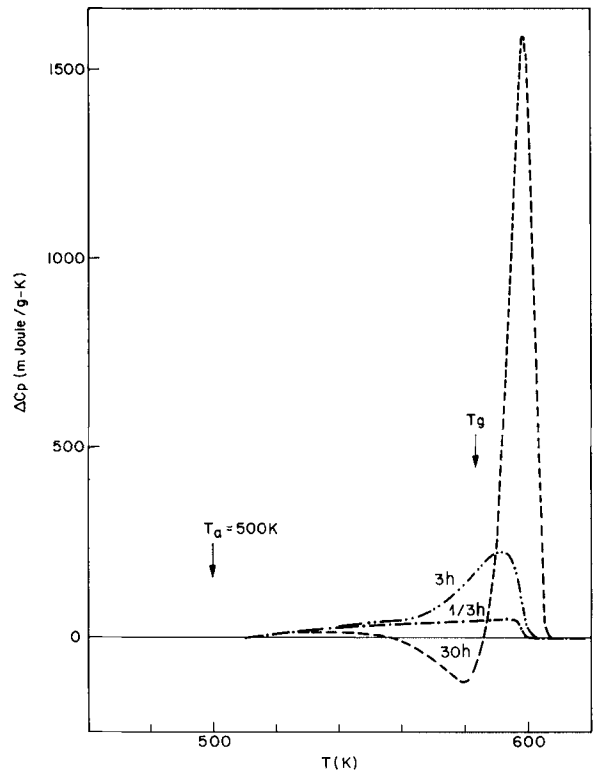


Fig. 9. Evolution of ΔC_p at $T_a=500$ K.

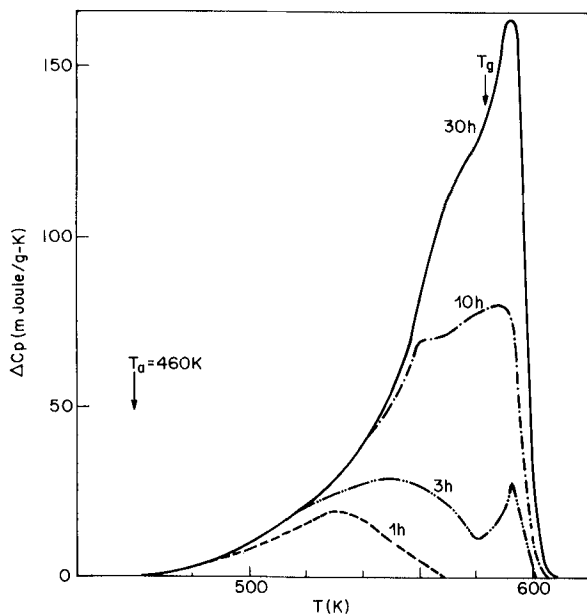


Fig. 8. Endothermic specific heat, ΔC_p , as a function of annealing time t_a , at $T_a=460$ K.

at the glass transition. Figure 8 shows the evolution of enthalpy, $\Delta C_p (=C_p - C_{p,r})$, of samples annealed at 460 K. If the annealing time is < 2 h, e.g. $t_a=1$ h as shown in Fig. 8, the sample exhibits the characteristic ΔC_p appearing above $T_a=460$ K and diminishing below T_g . When the sample is annealed for 3 h, it shows a similar endothermic peak above 460 K, but extending further into the glass-transition region ($T > T_g$), together with the appearance of an additional ΔC_p peak. For longer annealing times of $t_a=10$ h and 30 h, these two ΔC_p peaks merge into a broad split peak. As in the case of the 420 K anneal, the peak temperature, T_m , for this 460 K anneal varies linearly with $\log t_a$, as shown in Fig. 7.

An important aspect of these sub-sub- T_g relaxations, however, concerns the stability of the B_2O_3 glass in terms of these relaxa-

tions. Since in B_2O_3 the sub-sub- T_g relaxation has a relatively small intensity, it should not be expected to have a substantial effect on the stability of the glass. However, glasses showing these sub-sub- T_g relaxations are not as stable as would be expected, because it is the low-temperature (the sub-sub- T_g) relaxation which dominates the structural stability. This is shown in Fig. 8 for samples annealed at 460 K (120 K below T_g) for only 30 h. When the ΔC_p recovery peak extends into the transition regime the topological long-range structural relaxation takes place, as evidenced by the appearance of the ΔC_p peak in the transition region.

(B) *Sub- T_g Anneals: $T_g - 100 \leq T_a < T_g$* : Annealing studies at 500 K are shown in Fig. 9. A broad endothermic reaction extending from 500 K through the glass transition is observed for anneals as short as $1/3$ h. For an annealing time of 3 h, the sample shows the preendothermic peak followed by a pronounced glass-transition peak. For a longer annealing time of 30 h, a pronounced delayed-relaxation phenomenon, characteristic of T_g behavior, can be seen. The annealed sample now shows the whole C_p curve shifted to higher temperature by ≈ 10 K, so that the ΔC_p curve shows a dip below T_g , followed by a very sharp glass-transition peak at higher temperature. When the annealing temperature is increased even closer to T_g , e.g. $T_a=540$ K (not shown), a pronounced delayed-relaxation phenomenon, characteristic of sub- T_g anneal, is seen even for the shortest annealing time of 10 min.

(3) Activation Energies $Q_s(T_m)$ of Enthalpy Relaxation

If we associate the ΔC_p peak at T_m (or T_m') with a relaxation entity, an apparent activation energy, $Q_s(T_m)$, can be evaluated from isothermal annealing studies or from the shift of the ΔC_p peak with scanning rate measurements if the sub-sub- ΔC_p peak is well separated from the T_g peak.¹³ In the present measurements of amorphous B_2O_3 , the C_p peak is broad and thus T_m is not well defined. In addition, the limited amount of data in Fig. 7 is not sufficient and therefore the time-temperature shift method is used here. In this procedure, the sample is cooled through T_g before undergoing a low-temperature anneal. The annealed sample is heated to obtain the ΔC_p peak. The apparent activation energy (Q_s) is then approxi-

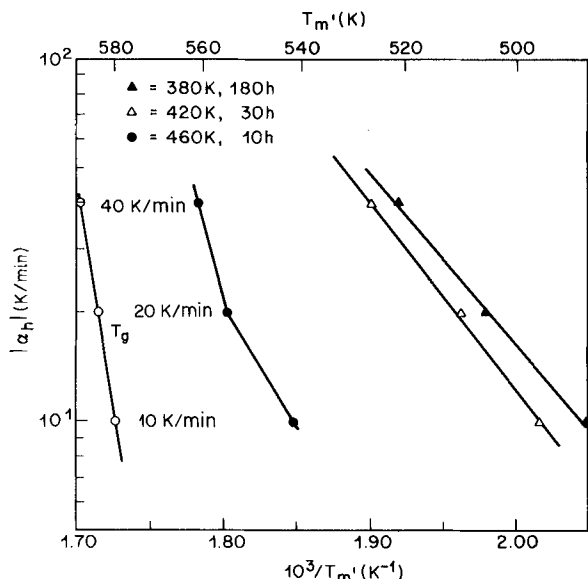


Fig. 10. Effect of heating rate, α_h , on T_m' and T_g .

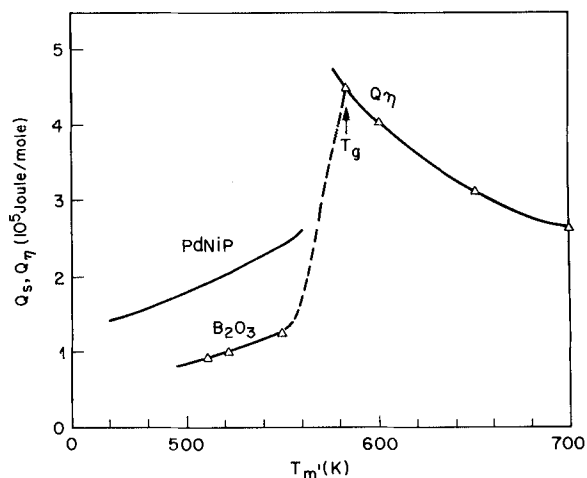


Fig. 11. Activation energies, $Q_s(T_m')$, of B_2O_3 glass; activation energies for viscous flow, Q_η (Ref. 14), are also shown (Δ).

mated from the shift of $\Delta C_p(T)$ curve or peak position with heating rate according to

$$[Q_s(T_m)/k_B T_m^2] = (d \ln \alpha_h) / dT_m \quad (4)$$

In the present investigation we used a value of $\alpha_c/\alpha_h = 4$ to increase the resolution of T_m (i.e. T_m' , as shown in Fig. 6). As shown in Fig. 10, the samples annealed at 380 and 420 K obey an Arrhenius temperature dependence quite well, but show a peak position dependence on t_a as well as α_h . The sample annealed at 460 K, in which the exothermic reaction exists over the transition region, shows a curvature in the $\log \alpha_h$ vs $1/T_m'$ relation. The observed T_g in the present case was seen to be independent of the annealings. $Q_s(T_m)$ varies from 10^5 J/mol at $T_m' = 510$ K to 1.3×10^5 J/mol at $T_m' = 550$ K, as shown in Fig. 11. As T_g represents the temperature at which relaxation time $\tau = \tau^*$, $Q_s(T_m)$ would connect $Q_g = 4.5 \times 10^5$ J/mol at T_g , where τ^* is the time constant of the measurement and is given³ as $\approx k_B T^2 / Q\alpha$ (≈ 10 to 40 s for $\alpha_h = 20$ K/min). Q_s thus would increase rapidly from 1.3×10^5 J/mol at 550 K to $Q_g = 4.5 \times 10^5$ J/mol at T_g .

The reported activation energies $Q_\eta(\Delta)$ of viscous flow¹⁴ are also shown in Fig. 11. Q_η decreases with increasing temperature, i.e. follows the Vogel-Fulcher relation. The present $Q_g(T_g) = 4.5 \times 10^5$ J/mol is in fair agreement with $Q_\eta(T_g) = 4.3 \times 10^5$ J/mol. For comparison, the Q_s values for Pd₄₈Ni₃₂P₂₀ alloy glass³ are also shown in Fig. 11. The metallic glass shows Q_s values twice that of the B_2O_3 glass, although both glasses exhibit the same values of $T_g = 583$ K and $Q_g(583 \text{ K}) = 4.5 - 4.8 \times 10^5$ J/mol.

If we assume a first-order process, the frequency factor ν_0 is evaluated as

$$\log \nu_0 \tau^* = Q_s / 2.3 k_B T_m \quad (5)$$

and is found to vary from $\approx 10^9$ to 10^{11} s^{-1} for $510 \text{ K} \leq T_m' \leq 550 \text{ K}$. These ν_0 values for the B_2O_3 glass are somewhat lower than but close to Debye frequency $\nu_D \approx 10^{12} \text{ s}^{-1}$. This contrasts with the very large $\nu_0 = (10^{16} \text{ to } 10^{22}) \text{ s}^{-1}$ found for the PdNiP glass at a corresponding temperature.

The relaxation spectrum $H(\log \tau)$ for the sub-sub- T_g anneals can be approximated from the enthalpy recovery measurements (Fig. 6) and activation energy Q_s . In the present case of a broad distribution in Q_s , neglecting the variation in ν_0 , the endothermic $\Delta C_p(\tau)$ peak would represent $H_L(Q \approx a k_B T)$,^{3,13} the portion of the initial activation energy spectrum $H(Q)$ which, during the anneal, has undergone the recoverable enthalpy relaxation, where a (≈ 25) is a constant. The relaxation spectrum $H_L(\log \tau)$ can then be obtained by merely converting the Q (or T) coordinate into a $\log \tau$ coordinate such that

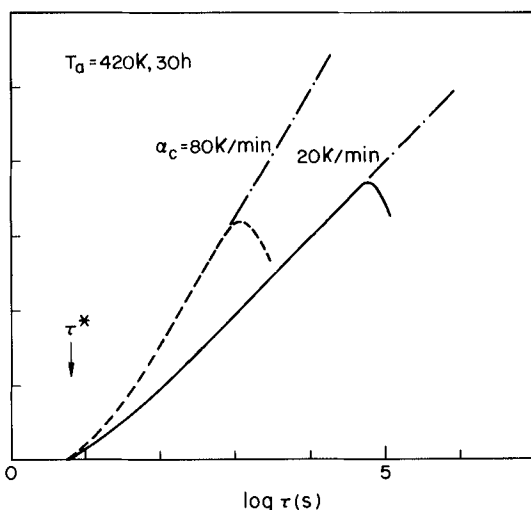


Fig. 12. Portion (short-time localized) of relaxation spectrum, $H_L(\log \tau)$ unnormalized.

$$\log \frac{\tau}{\tau^*} = \frac{Q_s(T)}{2.3 k_B T} \left(\frac{T}{T_a} - 1 \right) \quad (6)$$

The unnormalized $H_L(\log \tau)$ spectra for $T_a = 420$ K are shown in Fig. 12. The relaxation spectrum $H_L(\log \tau)$ spans at least four decades in relaxation time.

Structural relaxation of nonmetallic glasses near the glass transition has been investigated extensively for some time. The relaxation kinetics are often analyzed in the framework of a distribution in relaxation times ($\ln \tau$). In the following, we examine the applicability of the analysis used fairly successfully for the sub- T_g anneal to the sub-sub- T_g anneal. We will state briefly the analytical procedures commonly used. In practice, the following expressions are often used^{6,7}:

$$\rho - \rho_\infty = (\rho_0 - \rho_\infty) \exp \left[- \left(\int_0^t dt / \tau \right)^\beta \right] \quad (7)$$

$$\tau = A \exp \left[\frac{x \Delta h^*}{k_B T} + \frac{(1-x) \Delta h^*}{k_B T_f} \right] \quad (8)$$

where ρ_0 , ρ and ρ_∞ are values of properties at time $t=0$, t , and ∞ , respectively, and β ($0 \leq \beta \leq 1$), A , x ($0 \leq x \leq 1$), and Δh^* are constants. The Δh^* parameter can be obtained separately at equilibrium, i.e. $T \rightarrow T_f$. Equation (8) takes account of the nonlinear behavior. The relaxation function $\phi(t, \tau, \beta)$ in Eq. (7) corresponds

to the relaxation time spectrum $H(\ln \tau)$ with a peak in the distribution near $(\ln \tau)$ and being skewed toward shorter times. The smaller is the β value, the broader is the width of the distribution spectrum. When $\beta=1$, an exponential single relaxation obtains. Debolt *et al.*,⁷ from the analysis of enthalpy relaxation of B_2O_3 in the glass region, obtained $\Delta h^*=4 \times 10^5$ J/mol, $A=1.5 \times 10^{-33}$, $\beta=0.65$, and $x=0.40$ for the best fit of the data.

The Δh^* value of 4×10^5 J/mol is in fair agreement with our value of 4.3×10^5 J/mol. The other limiting value of activation energy, the isoconfigurational activation energy $\Delta h_T \left(\equiv k_B \frac{d \ln \tau}{d(1/T)} \Big|_{T_i=x\Delta h^*} \right)$, gives a value of 1.6×10^5 J/mol. However, present data for the low-temperature anneal, $\Delta h_T \leq Q_s = 1.0 \times 10^5$ J/mol to 1.3×10^5 J/mol $\leq x \Delta h^*$, as $d(1/T)/d(1/T) > 0$ (Figs. 4 and 5). This gives $x \leq 0.25$, which is much smaller than the value observed at the transition region for B_2O_3 ($x=0.40$) and other glassy materials ($x=0.50$).¹⁵

Although the β parameter cannot be evaluated without actually fitting the result with Eqs. (7) and (8), considering the distribution of short times extending over four decades would give an approximate value of $\beta \leq 0.30$. These x and β values are much smaller than those reported for sub- T_g relaxation studies of many glassy systems.¹⁵ Berens and Hodge¹⁶ reported similar endothermic ΔC_p recovery peaks below T_g in the low-temperature annealing of some glassy polymers. They were able to make reasonable, though not perfect, quantitative fits of their sub-sub- T_g data using Eqs. (7) and (8). However, the best fits require values of x and $\beta=0.2$ to 0.3 , which are too low as compared with the data for sub- T_g relaxation processes. Apparently the β distribution is not adequate to describe $H(\ln \tau)$, which has an asymmetric distribution skewed very heavily toward shorter times. In addition, the Δh^* values of 12.5×10^5 J/mol are physically unrealistic compared with values of $\approx 5 \times 10^5$ J/mol obtained separately at equilibrium.

(4) Possible Structural Models

The relaxation phenomena found here (e.g. the recovery on heating of the enthalpy relaxation incurred during the sub-sub- T_g anneal, the continuous enthalpy evolution with annealing time as seen in the recovery process, and gradual transformation of the sub-sub- T_g behavior to that characteristic of the sub- T_g anneal sample as the annealing temperature moves closer to T_g) were also found for metallic glasses^{1,3,4} and amorphous polymers.² These glassy materials phenomenologically appear to share many common features, although there exist some quantitative differences among the different glassy systems because of the striking differences in structural packing. We noted that the recovery process was greater in magnitude in metallic glasses and glassy polymers than in the B_2O_3 glass.

The most obvious characteristic of the distribution function required to account for the behavior seen is its extreme width—a very long short-time tail. As indicated earlier, however, from the results of Berens and Hodge it appears that a β distribution is not quite of the proper form to completely fit both sub-sub- T_g and sub- T_g relaxations at the same time. Although a simple bimodal distribution can obviously be fashioned to fit the experimental data, there seems to be no real evidence for this. The use of a model based on the framework of percolation theory has been proposed.³ The model assumes that (1) the structure of a glass and a liquid is inhomogeneous, with the inhomogeneity arising in monatomic materials from fluctuations in density, and in alloys from concentration fluctuations as well. It is visualized^{17,18} that a glass consists of liquidlike regions of large free volume or high local free energy, and solidlike regions with small free volume or low free energy. (2) Each region undergoes infrequent transitions between local minima well separated by energy barriers in configurational space.

The relaxation spectra thus are very broad and may be described by a β -distribution peak but more skewed toward short times (see Fig. 11 of Ref. 3). At high temperatures, $T > T_g$, every region in the whole system undergoes frequent configurational transformations and is liquidlike. During the cooling, the whole spectrum shifts to longer times, such that small portions of regions with $\tau > \tau^*$ are frozen-in and behave as isolated solidlike clusters embedded in a

liquidlike matrix. As the temperature approaches T_g , the solidlike clusters increase in number (e.g. a fraction of $t \approx 1/4$)¹⁹ and grow in size to such an extent that an infinite cluster surrounded by a liquidlike matrix is formed. This results in a drastic decrease in macroscopic flow and liquid-glass transition occurs. The glass transition $T_g(\tau^*)$ is then related to a percolation process. The relaxation processes near T_g are thus cooperative in nature. At a lower temperature, e.g. $T \leq T_g - 100$ K, the solidlike regions grow and the fraction of liquidlike regions decrease to below the percolation limit t' ($\approx t$). The liquidlike regions now are isolated from each other and are embedded in the rigid matrix. Relaxation then occurs locally in the liquid regions independent from each other. This model leads to localized modes of relaxation in sub-sub- T_g anneal and, on heating, the glass recovers the initial state without reheating through T_g . Accordingly, we may expect that these sorts of structural and compositional fluctuations are more pronounced in metallic and polymeric systems than in the network-type structure of B_2O_3 . The pronounced structural fluctuation in the former systems may also be reflected by the large anelastic behavior in the glass-transition regime.²⁰ At present, we cannot identify the underlying atomic mechanisms responsible for the localized modes of structural relaxation in B_2O_3 . However, based on the small activation energies $Q_s = 1 - 1.3 \times 10^5$ J/mol, and the closeness of the vibrational frequency $\nu_0 = 10^9$ to 10^{11} s⁻¹ to the Debye frequency $\nu_D = 10^{12}$ s⁻¹, the low-temperature structural relaxation in B_2O_3 is quite distinct, involving only a few atoms.

A model for B_2O_3 glass which seems to be generally accepted is one in which the oxygens are two-fold-coordinated with borons, the borons are three-fold-coordinated with oxygens, but some exist as isolated BO_3 triangles, whereas most are arranged in 3-triangle boroxol groups. Changes in temperature or pressure have been found to produce structural changes which can be interpreted as a breakdown of these boroxol groups, with the resultant formation of more randomly oriented BO_3 groups.

A second possibility which might account for the required fluctuations is related to the presence of small amounts of "dissolved" water. Both mechanical (330 K at 20 MHz) and dielectric (200 K at 30 kHz) measurements show a loss peak with an activation energy of 0.25×10^5 J/mol, which is associated with the presence of OH. Clearly, the relaxation process observed in this investigation occurs at a higher temperature, lower frequency, and with a higher activation energy so that the mechanism cannot be the same. However, the presence of the water may cause local density fluctuations allowing localized relaxation.

IV. Summary and Conclusions

We have shown that B_2O_3 glass undergoes a significant degree of structural relaxation when annealed at temperatures well below T_g ($T < T_g - 100$ K). This relaxation is accompanied by a decrease in enthalpy. The annealed samples show a gradual structural recovery on heating above T_a and a recovery of the initial enthalpy before the sample reaches T_f . The same calorimetric behavior found in the sub-sub- T_g anneal would be seen for samples annealed at higher temperatures, but still below T_g , e.g. $T_a = 500$ K, if the annealing times were very short. However, as T_a is increased to near T_g , a delayed C_p peak characteristic of sub- T_g anneals begins to appear at the transition.

In spite of very great differences in structure and bonding, the sub-sub- T_g relaxations found here are qualitatively similar, though smaller in magnitude, to those found in the polymeric and metallic glasses studied earlier.

It may be concluded from experimental data that B_2O_3 exhibits a very broad monotonic distribution of relaxation times. The relaxation spectrum consists of an asymmetric β distribution around a main peak and a long tail in the short times. In the framework of percolation theory, the short relaxation time is associated with the short-range localized structural relaxation (SLSR), whereas the main distribution peak accounts for the long-range cooperative structural relaxation (LCSR) commonly observed near T_g . It may be emphasized that the existence of the SLSR does not invoke a bimodal distribution of relaxation times.

Acknowledgment: H. S. Chen thanks I. M. Hodge for sending preprints of papers on the studies of glassy polymers.

References

- ¹H. S. Chen, "Kinetics of Low Temperature Structural Relaxation in Two (Fe-Ni)-Based Metallic Glasses," *J. Appl. Phys.*, **52** [3] 1868-70 (1981).
- ²H. S. Chen and T. T. Wang, "Sub-sub- T_g Structural Relaxation in Glassy Polymers," *J. Appl. Phys.*, **52** [10] 5898-5902 (1981).
- ³H. S. Chen, "On Mechanisms of Structural Relaxation in a Pd₄₈Ni₃₂P₂₀ Glass," *J. Non-Cryst. Solids*, **46**, 289-305 (1982).
- ⁴H. S. Chen, "A New Aspect of the Glass Transition Process and Structural Relaxation in Metallic Glasses"; pp. 495-500 in Proceedings of the 4th International Conference on Rapidly Quenched Metals, Sendai, 1981. Edited by T. Masumoto and K. Suzuki. The Japan Institute of Metals; Sendai, 1982.
- ⁵S. B. Thomas and G. S. Parks, "Studies on Glass—VI. Some Specific Heat Data on Boron Trioxide," *J. Phys. Chem.*, **35**, 2091-2111 (1931).
- ⁶C. T. Moynihan, A. J. Easteal, M. A. DeBolt, and J. Tucker, "Dependence of the Fictive Temperature of Glass on Cooling Rate," *J. Am. Ceram. Soc.*, **59** [1-2] 12-16 (1976).
- ⁷M. A. DeBolt, A. J. Easteal, P. B. Macedo, and C. T. Moynihan, "Analysis of Structural Relaxation in Glass Using Rate Heating Data," *J. Am. Ceram. Soc.*, **59** [1-2] 16-21 (1976).
- ⁸C. T. Moynihan, "Theory and Experimental Investigation of Structural Relaxation in Glass," *Wissen-Zeit., Friedrich-Schiller-Univ.*, **28** [2/3] 493-506 (1979).
- ⁹P. B. Macedo and A. Napolitano, "Inadequacies of Viscosity Theories for B₂O₃," *J. Chem. Phys.*, **49** [4] 1887-95 (1968).

- ¹⁰C. R. Kurkjian and J. T. Krause, "Effect of OH Content on the Acoustic Spectra of B₂O₃ Glass," *J. Am. Ceram. Soc.*, **49** [3] 171-72 (1966).
- ¹¹K.-H. Karsch and E. Jenckel, "Thermal and Mechanical Investigations of Alkali Borate Glass," *Glastech Ber.*, **34** [8] 397-408 (1961).
- ¹²W. Capps, P. B. Macedo, B. O'Meara, and T. A. Litovitz, "Temperature Dependence of the High Frequency Moduli of Vitreous B₂O₃," *J. Chem. Phys.*, **45** [9] 3431-38 (1966).
- ¹³W. Primak, "Kinetics of Processes Distributed in Activation Energy," *Phys. Rev.*, **100**, 1677-89 (1955).
- ¹⁴A. Napolitano, P. B. Macedo, and E. G. Hawkins, "Viscosity and Density of Boron Trioxide," *J. Am. Ceram. Soc.*, **48** [12] 613-16 (1965).
- ¹⁵C. T. Moynihan, P. B. Macedo, C. J. Montrose *et al.*, "Structural Relaxation in Vitreous Materials," *Ann. New York Acad. Sci.*, **249**, 15-35 (1976).
- ¹⁶(a) A. R. Berens and I. M. Hodge, "Effect of Annealing and Prior History on Enthalpy Relaxation in Glassy Polymers. I. Experimental Study on Poly(vinylchloride)," *Macromolecules*, **15**, 756-61 (1982).
- (b) I. M. Hodge and A. R. Berens, "II. Mathematical Modeling," *Macromolecules*, **15**, 762-770 (1982).
- (c) I. M. Hodge and A. R. Berens, "III. Experimental and Modeling Studies of Polystyrene"; unpublished work.
- ¹⁷M. H. Cohen and G. S. Grest, "Liquid-Glass Transition, a Free-Volume Approach," *Phys. Rev. B*, **20** [3] 1077-98 (1979).
- ¹⁸M. Cyrot, "On the Liquid Glass Transition," *J. Phys. Colloq.*, **41** [C8] 107-109 (1980).
- ¹⁹V. K. S. Shante and S. Kirkpatrick, "An Introduction to Percolation Theory," *Adv. Phys.*, **20**, 325 (1971).
- ²⁰H. S. Chen and M. Goldstein, "Anomalous Viscoelastic Behavior of Metallic Glasses of Pd-Si-Based Alloys," *J. Appl. Phys.*, **43** [4] 1642-48 (1972).

Chemical Analysis of Bi-Containing Magnetic Bubble Garnet Films

L. C. LUTHER and T. Y. KOMETANI

Bell Laboratories, Murray Hill, New Jersey 07974

Elemental compositions of Bi-containing garnet films suitable for 4 μ m period magnetic bubble devices were determined by gravimetric and atomic spectroscopic techniques. The analytical results were found to be in substantial agreement with estimates from material property measurements and, in particular, to validate a method of estimating Bi content from Faraday rotation measurements alone. Both Pb and Pt were found to be present at concentrations of 0.02 ± 0.01 atoms per formula unit.

I. Introduction

MANY properties of garnet materials vary in a simple linear manner with substitutional changes. This is most accurately true for lattice constants, magnetic moments, and ferromagnetic resonance line widths with substitution in the dodecahedral sublattice. Often substitutions in the iron lattices bring about changes which require second-order constants. But where such first- and second-order constants are known, good predictions of material properties can be made. Conversely, if the constituents of a garnet material are known, measurement of various material properties, especially lattice constants, FMR line widths, Curie temperatures, and magnetic moment, can be used to obtain quantitative information about material composition. Thus a surprisingly large amount of development can and has been done without the benefit of quantitative analyses which in general are difficult to obtain for the small amounts of material available with thin-film epitaxy.

In the development of garnet materials containing elements for which data are scarce and uncertain, the need for chemical analyses becomes more critical. In the exploratory phases of development of Bi-containing materials it was expedient to rely on lattice con-

stant and Curie-temperature data to characterize (YLuBi)₃Fe₅O₁₂ garnets with respect to Bi content, but some uncertainty remained because corrections had to be applied for the presence of Pb and octahedral rare earths. Supportive analytical data were available from X-ray fluorescence taken using SEM, but in the absence of strictly comparable standards these results could not be made quantitative.¹

Atomic absorption spectrometry (AAS) was recently used with good results to analyze magnetic materials.^{2,3} This method, as well as inductively coupled plasma emission spectrometry⁴ (ICP), was used to determine the composition of magnetic bubble film on a series of films which are thick by bubble film standards so as to make available samples of 100 mg or more. Thick layers also minimize effects of transient layers. For this work the film composition was chosen on the basis of the following criteria: (1) the film must, as far as possible, be comparable to Bi-containing bubble films, especially with respect to Bi content, (2) the composition should contain as few elements as possible, (3) the film lattice constant must match closely that of the only garnet substrate available in quantity, viz gadolinium gallium garnet (GGG), and (4) the film should not contain Gd or Ga to avoid complications arising from sampling the substrate. With respect to condition 3, the lattice match had to be better than the often-quoted margin of 0.002 nm because the desired films were to be unusually thick. The nominal composition chosen was (Y_{1.8}Bi_{0.6}Ca_{0.6})(Fe_{4.4}Si_{0.6})O₁₂, which is similar to that of films supplied for 4 μ m period device development work.

Bismuth has a very pronounced effect on Faraday rotation and for that reason this effect could be used to measure Bi content. One problem is that Pb is usually present and contributes to the Faraday rotation. For wave lengths between 550 and 700 nm the contribution of Pb per atom to the Faraday rotation is near 50% of that of Bi.⁵ Unless Pb is present in much smaller amounts than Bi this contribution cannot be ignored. Our previous work¹ supported the belief that the Pb content was an order of magnitude lower than the